Fabrication and Characterization of Advanced Triple-junction Amorphous Silicon Based Solar Cells

PHASE III – Quarter 3

Quarterly Technical Progress Report

SEPTEMBER 1, 2007 to November 30, 2007

NREL Subcontract No. ZXL-5-44205-06

Subcontractor: The University of Toledo

Principal Investigator: Xunming Deng
(419) 530-4782; dengx@physics.utoledo.edu

Co-Principal Investigator: Robert W. Collins
(419) 530-2195; rcollins@physics.utoledo.edu

Department of Physics and Astronomy
University of Toledo, Toledo, OH 43606

Contract technical monitor: Dr. Bolko von Roedern

Table of Contents

Cover Page

Table of Contents

Section 1: Executive Summary

Section 2: Study of amorphous silicon germanium solar cells with i-layer deposited at high rates using RF-PECVD

Section 3: Theoretical analysis and modeling of light trapping in a-Si based thin film solar cells

Section 4: Effect of ZnO deposition condition for back reflector on the performance of nano-crystalline silicon solar cell

Section 1

Executive Summary

This quarterly technical progress report covers the highlights of the research activities and results on the project of "The Fabrication and Characterization of High-efficiency Triple-junction a-Si Based Solar Cells" at the University of Toledo for the Period of September 1, 2007 to November 30, 2007, under NREL TFPPP subcontract number ZXL-5-44205-06.

Following this Executive Summary are the sections performed during this quarter related to the tasks under this subcontract. The major technical progresses of these sections are summarized as follows:

Section 2: Study of amorphous silicon germanium solar cells with i-layer deposited at high rates using RF-PECVD

The RF PECVD rate for a-Si:H intrinsic layer is usually low. The goal of this work is to explore alternative deposition conditions that may yield higher a-Si:H growth rate, while maintaining stable film properties. For this purpose, high rate intrinsic amorphous silicon germanium layers were deposited at low pressure 0.6 Torr and high pressure 2 Torr using frequency (RF) plasma enhanced chemical vapor deposition (PECVD) process. The deposition rate ranged from 2A/s to 10A/s. High rates were obtained mainly by increasing RF-power under both pressure settings. Initial efficiencies about 10% were available on single solar cells fabricated using these materials made on Ag/ZnO covered stainless steel substrate, while the light induced degradation for 110 hours was between 12% and 25%. Fourier transform infrared spectrometry was measured on the series of sample to show the film microstructure changes. Device results and film properties revealed that a-SiGe with good performances was obtained with the i-layers deposited at 2 Torr and 5A/s. Solar cell device parameters were: Voc=0.8V, short circuit current = 19 mA/cm2, Fill Factor = 0.66, and the initial efficiency = 10% (AM1.5). On the basis of the high rate a-SiGe solar cell, tandem amorphous silicon/a-SiGe solar cells were fabricated with both active layer done at 5A/s, and the initial efficiency was about 12.5%. Light induced degradation on tandem solar cells was under test.

Section 3: Theoretical analysis and modeling of light trapping in a-Si based thin film solar cells

Due to the essential importance of back reflector (BR) in multi-junction thin film solar cells, we have been conducting intensive research in this field both theoretically and experimentally. In this work, we focus on analyzing the light trapping effect. We discover that the light path enhancement factor of cells with an ideal Lambertian back reflector (BR) could be as high as $n(n+1)^2$, instead of general quoted $4n^2$. The program PVOPTICS developed by NREL has been used to modeling the light trapping effect. It is found that 1) the texture angle is more critical than the texture height in determining the light trapping effect, but the latter of which was the

only mentioned parameter in general light trapping designs; 2) inserting a ZnO buffer layer can largely increase the Si absorption, while ZnO thickness does not affect the light trapping obviously, which were confirmed by experimental results; 3) different impacts of texture starting from a-Si/ZnO or ZnO/metal interface on light trapping effects are studied. For ZnO/Al BR, the texture starting from the a-Si/ZnO interface will lead to a larger absorption in the Si layer; while for ZnO/Ag BR, the texture starting from the a-Si/ZnO interface or ZnO/Ag interface leads to similar results.

Section 4: Effect of ZnO deposition condition for back reflector on the performance of nano-crystalline silicon solar cell

Following our theoretical analysis on ZnO-based back reflector (BR) for applications in a-Si:H based thin film solar cells, we conducted systematic experiments. In this report, we summarize our experimental results focusing on the optimization of the ZnO films. We deposited ZnO at different substrate temperatures in a range of 120 ~ 350 °C for back reflector (BR) with a structure of ZnO/Ag/Al/SS used in nanocrystalline silicon solar cells. AFM, XRD, SEM and optical transmittance were employed to analyze the structure of ZnO films. It was found that the nanocrystalline solar cells on the back reflector with ZnO film deposited at 120 °C had a lower fill factor (FF) and a lower short-circuit current density (Jsc), but a higher open-circuit voltage (Voc). This might be caused by the high fraction of amorphous phase in the nanocrystalline silicon film, which grew on the low temperature deposited ZnO film. But when the ZnO deposition temperature was increased to 280 °C, the nanocrystalline silicon solar cells had a lower yield. The reason for this was due to the formation of a large amount of ZnO nanocrystalline rods on ZnO surface. The optimized BR had contributed to the development of high efficient a-Si:H/a-SiGe:H/nc-Si:H n-i-p triple solar cells with an efficiency of 12.5%.

Section 2

Study of amorphous silicon germanium solar cells with i-layer deposited at high rates using RF-PECVD

Wenhui Du, Xianbo Liao, Xiesen Yang, Xianbi Xiang and Xunming Deng
Department of Physics and Astronomy, University of Toledo, Toledo, OH 43606, USA

INTRODUCTION

Good quality medium band gap a-SiGe:H solar cells made at high rates are of great interest for the high efficiency multi-junction solar cell fabrication. The materials phase is optimized through changing the RF power density and process pressure, to realize the materials growth in the protocrystalline regime. The materials made in the protocrystalline regime contain a predominant amorphous component possibly with a very small volume fraction of nano-crystalline inclusions and as a result exhibit unique optoelectronic properties. High quality a-SiGe:H materials and high performance solar cells can be obtained if the deposition parameters are optimized. In the research reported here, we investigated a-SiGe:H n-i-p solar cells with intrinsic layers deposited at a high deposition rate of 2-10 Å/s. By adjusting the i-layer deposition conditions, a-SiGe:H intrinsic layer were grown near the phase transition in protocrystalline region. The single junction device shows good IV performance at deposition rate of 5A/s, and light induced degradation for 100 hours is 13% for optimized solar cells. We also report that incorporated such medium band gap a-SiGe solar cells into tandem a-Si:H/a-SiGe:H solar cell, the efficiency reach 12.5% (AM1.5).

EXPERIMENTAL DETAILS

a-SiGe:H n-i-p single-junction solar cells were fabricated using RF-PECVD techniques in our UT multi-chamber load-locked deposition system. The SiGe:H i-layers were prepared at a high deposition rate up to 8 Å/s under different pressure at 0.6 Torr and 2 Torr and RF-power densities from 0.028W/cm2 to 0.7W/cm2. The typical substrate temperature was in the range of 200 to300 C. Hydrogen dilution ratio R=[H2]/[Si2H6] in the range of 20 to 100 has been used for i-layer optimizations. The gas flow ratio of [GeH4]/[Si2H6] is from 0.4 to 0.6. The doped n and p layers were prepared at low deposition rates of 1 Å/s under amorphous and protocrystalline growth conditions. After fabrication of the n-i-p single-junction structure, the cells were completed by depositing indium tin oxide (ITO) transparent conductive layers through a mask to serve as the front contacts. Standard RF magnetron sputtering deposition techniques were used for the ITO. Each cell has an active area of 0.25 cm2. For characterization of the as-deposited cells, standard dark current voltage (I-V) and AM1.5G light I-V measurements were made. Standard QE measurements were made in the wavelength range of 350 to 1000nm. Light-soaking experiments were undertaken with ~ 100 mW/cm2 white light at 50 C. Fourier transform infrared spectrometry was measured on films deposited on c-Si substrates, where amorphous sub-layer has been inserted before i-layer depositions.

RESULTS AND DISCUSSION

Figure 1 shows the FTIR spectra of 500 nm thick a-SiGe:H i-layer deposited on c-Si substrate. The spectrum is deconvoluted into three major peaks, located at 1877cm^{-1}, 2007 cm^{-1} and 2087 cm^{-1}, corresponding to the stretching modes of GeH, SiH and SiH2 bonds, respectively. The ratio of [GeH]/[SiH] and [SiH2]/[SiH+SiH2] are determined to describe the film property. Table 1 lists the ratios as well as the deposition parameters. Films deposited at low pressure region tend to have a small microstructure at a low power than those of high power, 0.22 compared to 0.4. While at high pressure region, the film quality is better at 30W compared to the ones of 12 W and 50 W. High power and high pressure conditions may reduce the quality by introducing more voids or clusters in the film. Amorphous SiGe:H solar cells have been fabricated using these different materials. Table 1 also shows the Voc of the solar cells and 110 hours light induced degradation (LID) results. It can be seen that LID factor is low for sample made at 10W at 0.6 Torr and 30W at 2 Torr. It should be noticed that the 2 Torr sample has a higher deposition rate than samples made at low power low pressure region. It indicate that the good quality SiGe materials is possible to be obtained at high pressure and high power region, which is believed to be close to transition region and to be protocrystalline.

Table 1 Deposition conditions, deposition rates, and the ratio of hydrogen in different modes for a-SiGe:H intrinsic layers; flow ratio of [GeH4]/ [Si2H6] is 0.4.

Sample #	Pr. (Torr)	R	Power (W)	Rd (A/s)	GeH /SiH	SiH2/ (SiH2+SiH)	Voc (V)	LID (%)
gd2442	0.6	50	10	2.3	0.29	0.24	0.793	14
gd2443			15	5.4	0.51	0.22	0.786	23
gd2447			30	4.9	0.59	0.40	0.791	23
gd2451			50	5.7	0.41	0.39	0.789	19
gd2469	2	100	12	2.3	0.52	0.34	0.774	-
gd2448			30	6.0	0.32	0.24	0.802	12
gd2450			50	7.7	0.19	0.48	0.844	15

In order to verify the results from film study and single junction devices, a-SiGe:H solar cells has been made on Ag/ZnO coved stainless steel and further tandem solar cell a-Si:H/a-SiGe:H has been fabricated. The I-V curves of the tandem cell are shown in figure 2 with Voc=1.77 V, Jsc=10.5 mA/cm2, F.F.=0.67, and efficiency=12.5% at AM1.5.

CONCLUSIONS

We have fabricated and optimized good performance medium band gap a-SiGe:H n-i-p solar cells with 5 Å/s intrinsic layers grown in protocrystalline phases, optimized through high pressure and high power conditions in RF-PECVD. Compared to the low pressure region deposition, high pressure increase not only deposition rate but material stability. The light

induced degradation is about 13% for optimized samples. On the basis of the high rate a-SiGe:H solar cells, a-Si:H/a-SiGe:H with the active layer fabricated at 5A/s can reach high initial efficiency of 12.5% (AM1.5). high-efficiency a-Si:H top or nc-Si:H bottom cells in tandem and triple-junction devices.

ACKNOWLEDGEMENTS

This research was supported by the National Renewable Energy Laboratory "Thin Film Photovoltaics Partnership Program" under subcontract No. ZXL-5-44205-06.

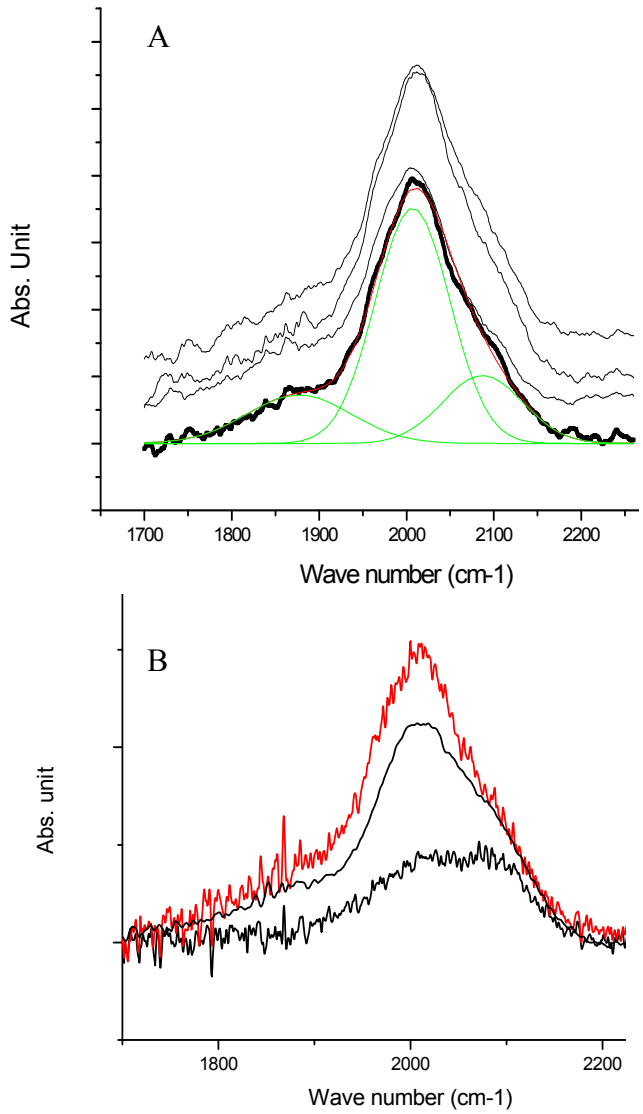

Figure 1A: FTIR spectra of a-SiGe:H film made at 0.6 Torr, power are 10W, 15W, 30W and 50W from the bottom to the top curve. Figure 1B is plotted for 2 Torr samples; power is 12W for bottom curve, 30W for red curve and 50W for middle one.

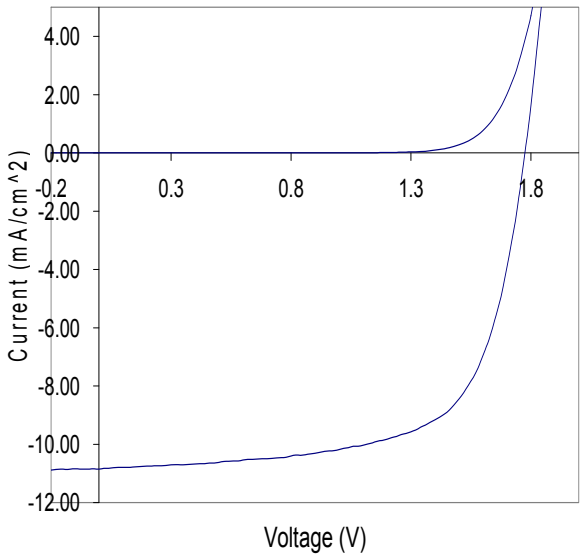

Figure 2, I-V curve of high rate tandem a-Si/a-SiGe solar cells.

Section 3

Theoretical analysis and modeling of light trapping in a-Si based thin film solar cells

Xiesen Yang, Xianbo Liao, Wenhui Du, Xinmin Cao, Dinesh Attygalle, Xianbi Xiang, Nirupama Adiga, and Xunming Deng
Department of Physics and Astronomy, University of Toledo, Toledo, OH 43606, USA

INTRODUCTION

For a-Si:H and nc-Si:H based thin film solar cells, light trapping is important to achieve a high efficiency by enhancing absorption, specially for the weakly absorbed long wavelength light [1, 2]. In an ideal light trapping regime, the light is repeatedly scattered and reflected in the solar cells and mostly absorbed within the intrinsic layer, where the photocurrent is generated [3, 4].

For instance, the amorphous silicon germanium (a-SiGe) alloy used in bottom component cell typically has an absorption coefficient of ~ 10^4 cm^{-1} at wavelength at approximately 700 nm [5]. This means the solar cell will require about 1000 nm to absorb 63% of the incident light at approximately the 700 nm wavelength range. But the holes typically have a drift length of ~ 0.1 μm and a diffusion length less than 0.1 μm [6]. The low drift length will make it difficult to collect the photo-generated carriers in a thick device. In our practice, the typical thickness of the a-SiGe bottom component cell is approximately 200 nm. Compared to the needed thickness of more than 1000 nm to efficiently absorb the incident light with a wavelength longer than 700 nm, the actual 200 nm thickness is not thick enough. Under these conditions, the device will need a light trapping design, which gives an effective light travel length at least 7 times larger than the absorbing layer thickness.

For solar cells deposited on stainless steel substrate, the light trapping effect is based on the high reflection and scattering at the rough back surface and the inner reflection at the front surface. This paper investigates the theory of light scattering and light trapping in the thin film solar cells with a rough BR, and uses PVOPTICS to model different light trapping designs.

THEORETICAL ANALYSIS AND MODELING

1. Theoretical Analysis

A simplified light trapping design with an ideal Lambertian BR used in thin film solar cells was proposed by Nelson [6], where he got the light path enhancement factor $\zeta = 4n^2-2 \approx 4n^2$, with assumptions that all the light reaching the front surface within the critical angle θ_c will escape. Following the method by Nelson, but considering the fact that only part of the light within the critical angle will escape from the front surface, one can get a larger light path enhancement factor, as shown in Fig. 1.

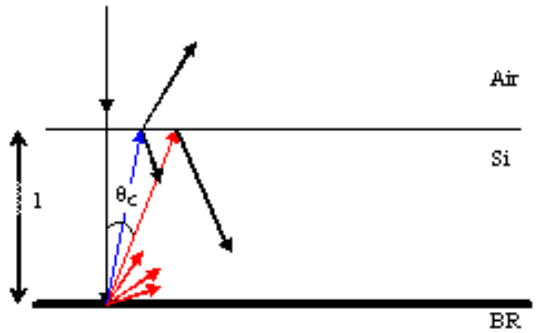

Fig. 1 *Lambertian back surface scattering increases light path in the medium.*

The normal incident light has a light path of 1 and arrives at the Lambertian back surface. For first order scattering of the perpendicular incident light, the mean light path from a flat back surface to the front surface will be only 1, while from a Lambertian BR, it will be 2, as calculated by equation (1),

$$\int_0^{2\pi} d\phi_s \int_0^{\pi/2} \sin\theta_s d\theta_s \frac{dP_s}{d\Omega_s} \frac{1}{\cos\theta_s} = \int_0^{2\pi} d\phi_s \int_0^{\pi/2} \sin\theta_s d\theta_s \frac{FP_i \cos\theta_s}{\cos\theta_s} = 2 \qquad (1)$$

From here we can see that the Lambertian back surface scattering reflection can double the light path compared to the specular surface reflection without counting the multi-reflection effect of light trapping.

When the first order scatter reflected light strikes on the front surface, it will be reflected by the front surface and only the portion with a small angle $\theta_s < \theta_c$ can partly escape from the cell. The ratio of the portion of light with this small θ_s to all the light reaching at the front surface is:

$$\int_0^{2\pi} d\phi_s \int_0^{\theta_c} \sin\theta_s d\theta_s \frac{dP_s}{d\Omega_s} = \int_0^{2\pi} d\phi_s \int_0^{\theta_c} \sin\theta_s d\theta_s FP_i \cos\theta_s = \sin^2\theta_c = \frac{1}{n^2} \qquad (2)$$

The transmission T_1 at the front surface is due to the partly escaping of the small θ_s light:

$$T_1 = \frac{4n}{(n+1)^2} \qquad (3)$$

with the assumption that θ_s within the critical angle is small, and that k is much less than n of the medium. So the actual loss, due to the partial escaping of the first order scatter reflected light with small θ_s at the front surface should be:

$$\frac{1}{n^2}\frac{4n}{(n+1)^2} = \frac{4}{n(n+1)^2} \qquad (4)$$

The rest of the first order scatter reflected light is totally reflected back into the medium. It will have a path of approximately 2 to get to the back surface. Then it will scatter reflect again at the back surface. It is assumed that the first pass is normal incident with a path length of 1 and all the back surface scattering reflection and front surface reflection has a pass length of 2 and the last light which satisfies $\theta_s < \theta_c$ will leave the cell with a pass length to be approximately 1. Adding up the path lengths of lights before they escape from the front surface, it is:

$$\frac{4}{n(n+1)^2}\times 2+\frac{4}{n(n+1)^2}\times(1-\frac{4}{n(n+1)^2})\times 6+\frac{4}{n(n+1)^2}\times(1-\frac{4}{n(n+1)^2})^2\times 10+\ldots \quad (5)$$

Summing the series to the infinite order, we get the light path enhancement factor ζ to be:

$$n(n+1)^2-2\approx n(n+1)^2 \quad (6)$$

This light path enhancement factor is larger than $4n^2$ as deduced by Nelson. For a-Si solar cells, this is about 100 for 800nm wavelength (n~4). This number is larger than $4n^2$ =~64. The larger result is due to the partial reflection of the light reaching at the front surface within the critical angle. It notes that this calculation does not account for the optical losses at the scattering back surface. In actual devices, these optical losses cannot be negligible.

2. Modeling by PVOPTICS

PVOPTICS program developed by NREL is used to modeling the optical properties of cells with different texture and configurations. The typical cell structure is ITO/p/i/n/ZnO/metal/substrate, with parameter settings as follows: ITO layer, n = 1.95, k = 0, d = 0.071 µm; a-Si layer, d = 0.3 µm; ZnO layer, n = 2, k = 0, d = 0.6 µm; Ag layer, d = 0.35 µm; texture height 0.1 µm, texture angle 30°. The modeling solar cell is a bottom cell with the i layer bandgap ~ 1.45 eV.

MODELING RESULTS AND DISCUSSIONS

1. Texture Height and Texture Angle

On ZnO/Ag back reflectors, the calculated maximum achievable current density (MACD) is shown in Fig. 2. The data points include texture height (rms roughness) ranging in 5, 10, 20, 35, 50, and 100 nm and texture angle ranging in 0, 10, 20, 30, 45, 60, and 80°.

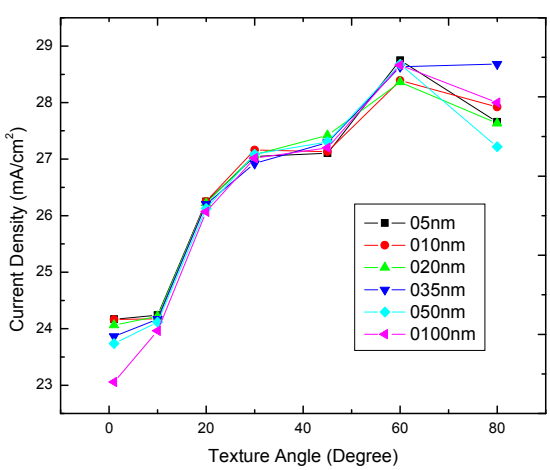

Fig. 2 *The MACD of bottom cell with ZnO/Ag BR at different texture heights (rms) and angles.*

This result shows that the texture height is not as critical as the texture angle in light trapping. Different texture height with same texture angle has about the same J_{sc}. This result agrees well with the rough surface scattering theoretical analysis by Beckmann[7].

The actual texture angles of Al and Ag films were measured by AFM. It was found that the maximum texture angles of Al and Ag films are ~ 28° and ~ 15° respectively, with same sputtering deposition conditions: Ar flow, 30 sccm; gas pressure, 5 mTorr; RF power, 100 W; substrate temperature, 400 °C; film thickness, 350 nm.

2. *ZnO Buffer and Thickness*

The ZnO layer works as a buffer layer in the device, it prevents the inter-diffusion between Ag and Si layers. Because sputtering deposited ZnO is normally porous, so in practice, it needs a thickness above 350 nm to effectively prevent the inter-diffusion. We calculated cell absorption with different ZnO thickness. Figs. 3 and 4 show the results about the absorption in Si and metal layers.

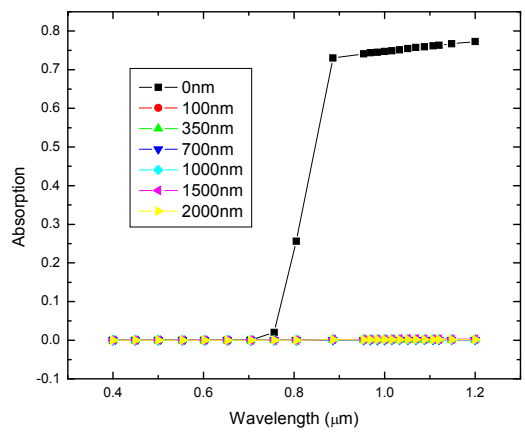

Fig. 3 *Metal Ag absorption losses of 2 μm thick bottom cells with different ZnO thicknesses.*

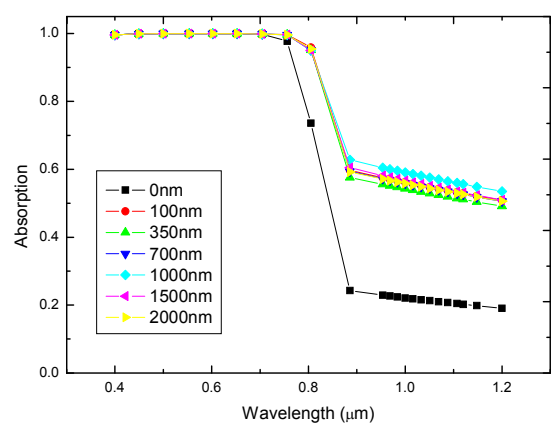

Fig. 4 *The Si absorptions of 2 μm thick bottom cells with different ZnO thicknesses.*

The results show that inserting a ZnO layer can increase the Si absorption, compared with a device without ZnO as the buffer layer. This may be due to the lower refractive index (2.0) of ZnO compared to Si (4 in the visible and near IR spectral range) and the increase of the reflection of BRs and the decrease of metallic loss. Sopori did a calculation with a lower refractive index (1.45) MgF_2 compared with ZnO as the buffer layer [8]. The results show an even larger MACD compared with ZnO. And the results here show that Si absorption is about the same with different thickness of ZnO ranging from 0.1 to 2 μm. This is due to the assumption k = 0 for ZnO.

To confirm the simulation results, complete solar cells were used to evaluate ZnO thickness effect. Four BRs were deposited with the same conditions except for the different ZnO thicknesses: 200, 350, 1200, 1500 nm. Then two nc-Si deposition runs (GD2168 and GD2169) were used to evaluate the BRs. Then, IV and QE of the cells were measured. The IV results are shown in Table 1. As can be seen that the short circuit current and other performances of the solar cells are about the same when ZnO films have a thickness of 200, 350, 1200, and 1500 nm. There is a little difference in the performances between sample GD2168 and GD2169, but this is due to the Si deposition, not from the ZnO thickness.

Table 1 The IV performance of nc-Si cells with different ZnO thicknesses (d).

Sample #	ZnO d (nm)	V_{oc} (V)	J_{sc} (mA/cm^2)	FF (%)	EF (%)	Yield --
GD2168-1,3	1500	.511	22.04	72.5	8.17	30/34
GD2168-2,4	200	.508	22.18	71.0	8.01	28/34
GD2169-1,3	1200	.505	22.41	70.3	8.32	23/34
GD2169-2,4	350	.502	22.07	71.3	8.26	17/34

The QE curves of GD2168 illustrated in fig. 5 show that the cell response in the entire wavelength range is about the same for the samples with ZnO thickness of 1500 and 200 nm. The experimental data agree well with the simulation results, and also confirms that our intrinsic ZnO films have very low optical absorption coefficients in the long wavelength range.

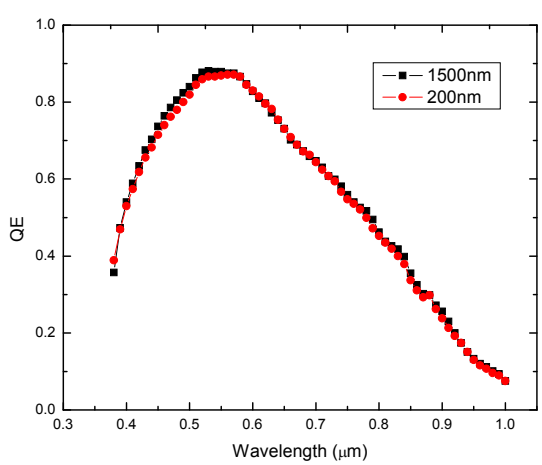

Fig. 5 *The QE curves of nc-Si cells GD2168 with different ZnO thicknesses.*

3. *Textured or Planar ZnO/Al Interface*

It is known that the textured interface will lead to better light scattering, but it will lead to more optical losses at the buffer/metal interface. It is possible to get the texture from the buffer layer by adjusting the deposition parameters or using chemical etching. PVOPTICS was also used to evaluate the two different texture designs.

The impacts of different ZnO/Al BRs on the Si absorption are shown in figs. 6. The results show that the textured buffer/metal interface improves the light trapping of the device. This is reflected by the higher total absorption in the case of textured buffer/metal interface than in the case of planar interfaces.

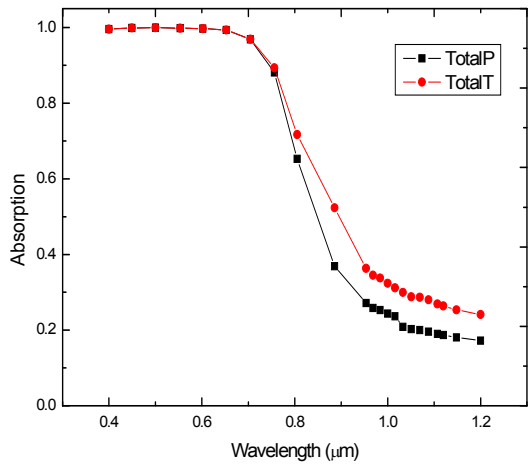

Fig. 6 Total absorption of bottom cells on ZnO/Al BRs with planar and textured ZnO/Al interfaces.

Fig.7 shows the absorption in Si layers and metal layers of bottom cells with planar and textured ZnO/Al interfaces. It can be seen that the absorption in the Al layer is larger when the buffer/metal interface is textured than when it is planar. By using the planar buffer/metal interface, the total light trapping effect is smaller, but the metal absorption is reduced more, so there is gain in the Si layer absorption. However, similar study on ZnO/Ag BR shows that the result is about the same for the two different texture designs.

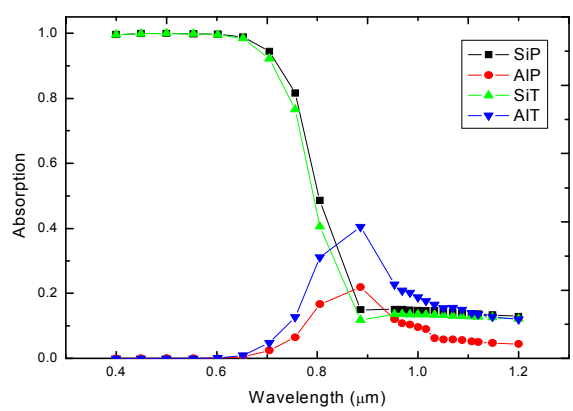

Fig. 7 The absorption in Si layers and metal layers of bottom cells with planar and textured ZnO/Al interfaces.

CONCLUSIONS

The ideal light trapping design has been analysed and the light path enhancement factor is found to be $n(n+1)^2$, instead of the generally accepted $4n^2$, with assuming that only part of the light reaching the front surface within the critic angle will escape. The modeling results by PVOPTICS show that the scattering property of the surface is mainly determined by its texture angle, not the texture height. The modeling result also says that the ZnO layer as a buffer layer is indispensable and the thickness does not affect the light trapping. For ZnO/Al BR, the texture starting from the a-Si/ZnO interface will lead to a larger absorption in the Si layer; while for ZnO/Ag BR, the texture starting from the a-Si/ZnO or ZnO/Ag interface leads to similar results.

ACKNOWLEDGEMENTS

This work was supported by the National Renewable Energy Laboratory "Thin Film Photovoltaic Partnership Program" under subcontract No. ZXL-5-44205-06.

REFERENCES

[1] H. W. Deckman, C.R. Wronski, H. Witzke and E. Yablonovitch, Appl. Phys. Lett. 42, 968 (1983).
[2] X. Deng, K. L. Narasimhan, First WCPEC; Dec. 5-9, 1994; Hawaii.
[3] N. Senoussaoui, T. Repmann, T. Brammer, H. Stiebig, H. Wagner, Rev.energ. ren. vol.3 (2000) 49-56.
[4] Pouya Valizadeh, Amorphous Silicon Solar Cells: Efficiency and Stability Issues.
[5] X. Deng and E. Schiff, "Amorphous Silicon Related Solar Cells', a chapter in Handbook of Photovoltaic Science & Engineering, eds. A. Luque & S. Hegedus, John Wiley & Sons Ltd., 2003.
[6] Jenny Nelson, The Physics of Solar Cells, Imperial College Press, ISBN 1-86094-340-3, 2003.
[7] P. Beckmann and A. Spizzichino, The Scattering of Electromagnetic Waves from Rough Surfaces, Pergamon Press, New York, 1963
[8] B. Sopori, etc., the materials research society's spring 99 meeting, San Francisco, California, April 5-9, 1999.

Section 4

Effect of ZnO deposition condition for back reflector on the performance of nanocrystalline silicon solar cell

Xiesen Yang, Xinmin Cao, Wenhui Du, Chandan Das, Yasuaki Ishikawa, Lauri Edwards,
Xianbo Liao, Xianbi Xiang, and Xunming Deng
Department of Physics and Astronomy, University of Toledo, Toledo, OH 43606, USA

INTRODUCTION

This work focuses on the optimization of ZnO as a part of back reflector (BR) for nano-crystalline (nc-Si:H) thin film solar cells. The purpose of the back reflector is to trap the photons of long wavelength and thus improve the current generated by the bottom cell [1, 2]. The BR nor-mally consists of highly reflective metal layer (Al or / and Ag) and ZnO buffer layer. It is important to optimize the texture of the BR to improve the light trapping [3, 4]. At the same time morphology of ZnO is also important since it acts as a direct substrate for the growth of Si thin film. It is known that the nc-Si:H microstructure is critically sub-strate-dependent [5]. The film morphology of ZnO is mainly determined by the deposition conditions of the sputter process [6]. Deposited at certain regime, although the ZnO films exhibit nearly similar transparency and re-sistivity, they show distinctly different surface morpholo-gies [4, 7].

This paper discusses the effect of deposition tem-perature of ZnO on film morphology and as a part of BR on the performance of nc-Si:H solar cell.

EXPERIMENTAL DETAILS

We fabricated BR's on stainless steel (SS) substrate by RF sputtering method. The complete structure of BR was ZnO/Ag/Al/SS. The Al and Ag metal layers, depos-ited at fixed conditions, providing high texture and high reflectance. The ZnO films were deposited at four differ-ent substrate temperatures (120, 200, 280, and 350 ºC), keeping other conditions such as RF power (100 W), Ar gas flow (4 sccm), chamber pressure (4X10-3 Torr) and deposition time (t = 50 mins) unchanged. The morpholo-gies of the BR's surfaces were characterized by Scanning Electron Microscopy (SEM). The ZnO single layer films deposited on 1737 glass substrate at different tempera-tures (25, 150, 250, and 320 °C) were measured by opti-cal transmittance for the optical properties, by Atomic Force Microscope (AFM) for the roughness, and by X-ray Diffraction (XRD) for their grain size.

Standard nc-Si:H n-i-p single junction solar cells were deposited on BRs with ZnO deposited at different temperatures to see the effect of BR on cell perform-ance. For comparison purpose we also fabricated n-i-p solar cell on control sample of BR (ZnO/Ag/SS). In addi-tion to this we also fabricated triple junction a-Si:H/a-SiGe:H/nc-Si:H n-i-p solar cell on BR with ZnO deposited at 280ºC. Cells were characterized by external quantum efficiency (QE) and J-V measurements.

RESULTS AND DISCUSSION

1. Optical Properties of ZnO

Figure 1 shows the transmittance of ZnO deposited at different temperatures. The ZnO film deposited at room temperature has lowest transmittance. The films deposited at 150 and 250 ºC have about the same transmittance. The film deposited at 320 ºC has lower transmittance again. This lower transmittance at high temperature may be due to the film high roughness, which will lead to haze. Film absorption coefficients as a function of photon energy are plotted in fig. 2. From it, the direct bandgap of ZnO is calculated as 3.282, 3.277, 3.277, and 3.275 eV for samples deposited at 25, 150, 250, 320 ºC, respectively, similar to the Burstein-Moss shift.

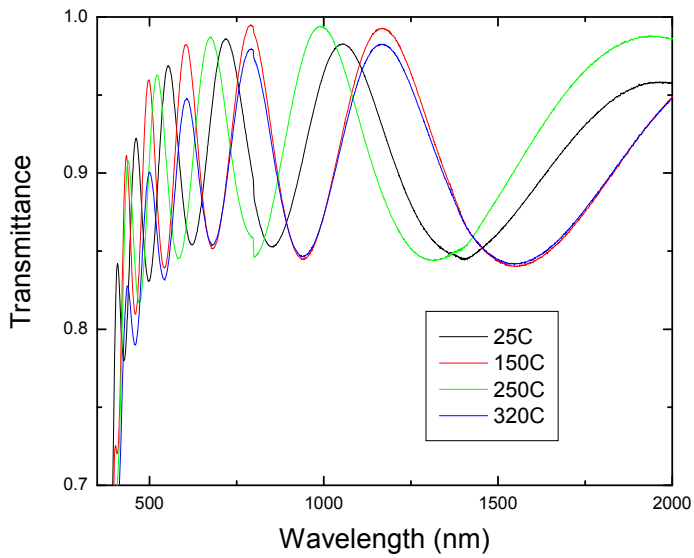

Fig. 1 The transmittance curves of ZnO samples deposited at different temperatures.

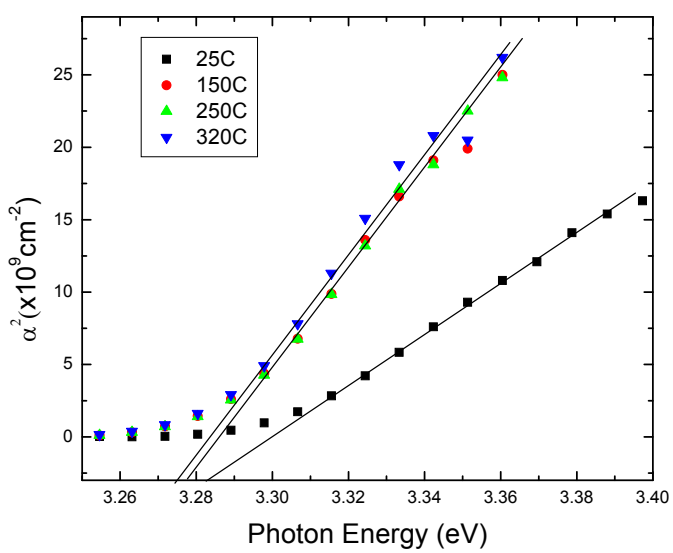

Fig. 2 Square of the absorption coefficient as a function of photon energy for the samples deposited at different conditions.

2. *Surface Characterization of BR*

Figure 3 shows the SEM images of the complete BR with ZnO deposited at different temperatures. The main feature size is about 1000 nm for all temperatures. All the BRs exhibit similar texture with nearly micron size features independent of the deposition temperature of ZnO. This feature is from the Al layer, which deposited underneath at the same condition. The smaller features in the 200 nm size are from ZnO crystalline clusters. The nano-rods growth is enhanced in terms of numbers and length, with increasing temperature from 120ºC (a) to 350°C (d). The SEM image of the BR with ZnO deposited at 350 ºC shows large number of crystallite ZnO rods with length larger than 1 micrometer. These crystallite ZnO rods can cause low yield problem of the nc-Si:H solar cells; so we do not have solar cells deposited on BR with ZnO deposited at 350 ºC.

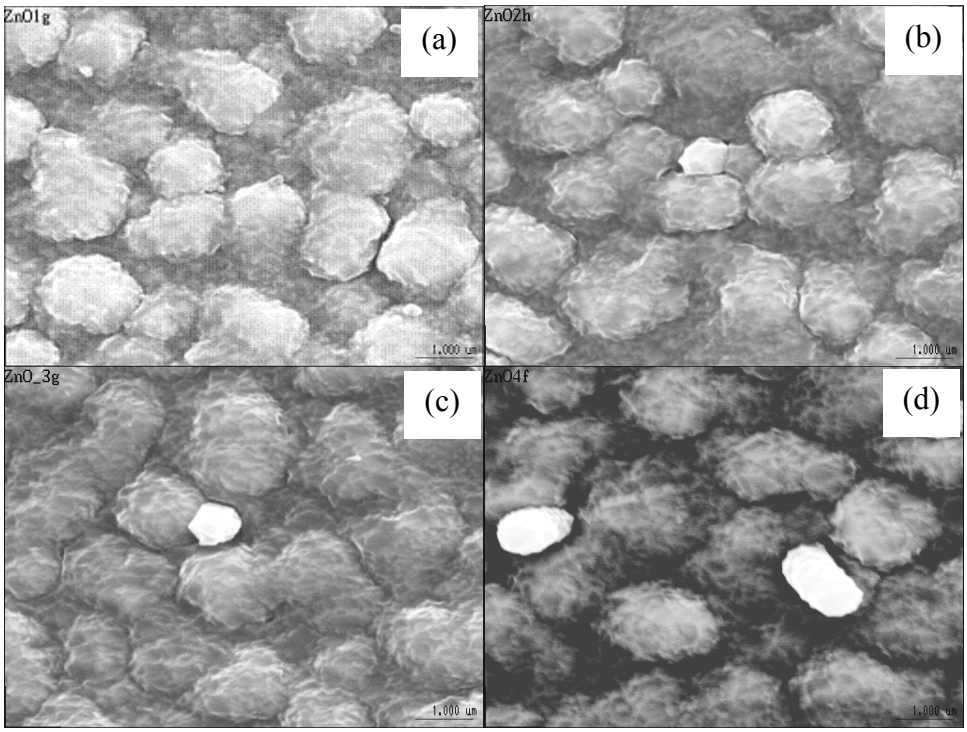

Fig. 3 The SEM image of ZnO films on top of Ag/Al. ZnO films deposited at (a) 120, (b) 200, (c) 280, (d) 350 ºC from top to bottom, respectively. The main feature size is from the Al layer. ZnO layer crystallinity is getting more and more obvious with increasing temperature. The nano-rods growth enhanced with increasing temperature.

On the other hand, morphology of ZnO films deposited at different temperatures is different, as measured by AFM, shown in Fig. 4. These ZnO films were deposited on 1737 glass substrate, their rms roughness increased from 7.4nm (a) to 17.2nm (d) with temperature from 25ºC to 320°C. The increase in rms roughness means the ZnO films have polycrystalline

structure and their crystallinity develops with increasing substrate temperature. The AFM images also show the 200 ~ 300 nm size clusters of grains.

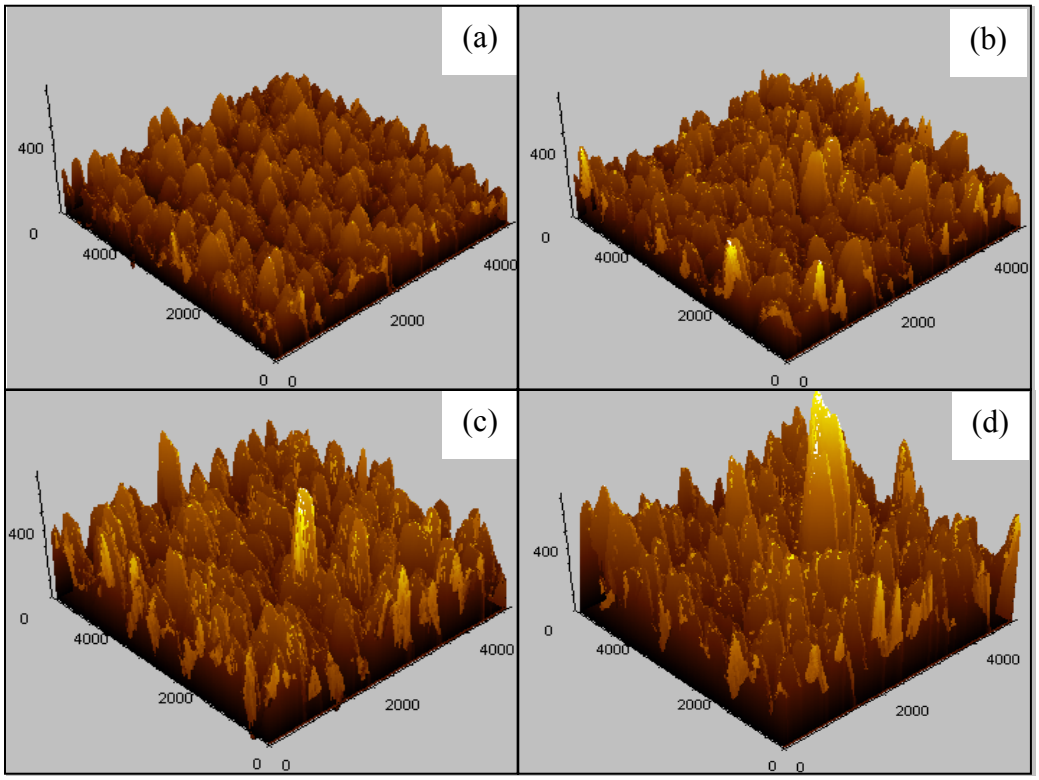

Fig. 4 AFM images of ZnO films deposited on glass at 25, 150, 250, 320 ºC from top to bottom. X and y scales are in nm, z scale is in Å.

We also used XRD to measure the grain size of the films. It is found that the grain size of the films is 24, 26.4, 27.7, and 28.3 nm for substrate temperature 150, 200, 250, and 320 °C, respectively. The AFM and XRD data show that the ZnO films crystallinity increases with deposition temperature.

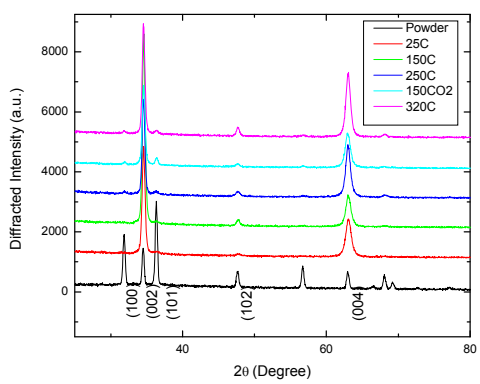

Fig. 5 The XRD pattern of ZnO films deposited at different conditions.

3. *Effect of BR on nc-Si:H Solar Cell*

To compare the cell performance and evaluate the quality of our BR, we deposited standard nc-Si:H solar cell on control sample, simultaneously with BRs fabricated here at the University of Toledo. Table 1 shows the J-V data of the above mentioned samples.

Table 1: *J-V data for nc-Si:H n-i-p single-junction cells on BRs with ZnO deposited at different temperatures and on control samples.*

Cell Nr.	T_{sub} (ºC)	V_{oc} (V)	J_{sc} (mA/cm^2)	FF (%)	η (%)
ZnO-1	120	0.541	17.1	52.6	4.86
Control	-	0.518	21.4	60.0	6.68
ZnO-2	200	0.510	22.8	61.9	7.20
Control	-	0.512	21.6	64.1	7.08
ZnO-3	280	0.526	20.6	64.3	6.96
Control	-	0.516	19.7	65.4	6.65

From the J-V data in table 1, we can see that the cell with ZnO deposited at 120 ºC, has low J_{sc} and low FF, but high V_{oc}. The low temperature deposited ZnO film on which the nano-crystalline silicon is deposited can explain this. As a result of the low temperature deposited ZnO, nano-crystalline silicon has more amorphous phase, which gives high V_{oc}, but low J_{sc} and low FF in cell performance. From table 1, we can see that the cells with ZnO deposited at 200 ºC and 280 ºC both have better performance than their control samples.

The QE data of sample ZnO-1 also show a low spectral response in short and long wavelength range. While sample ZnO-2 and ZnO-3 both have better spectral response than their control samples. The QE curve in figure 2 shows that cell with ZnO deposited at 200 ºC has a better spectral response in the long wavelength range than the control sample with ZnO/Ag BR. This means the BR made under this condition is suitable for nc-Si:H cells.

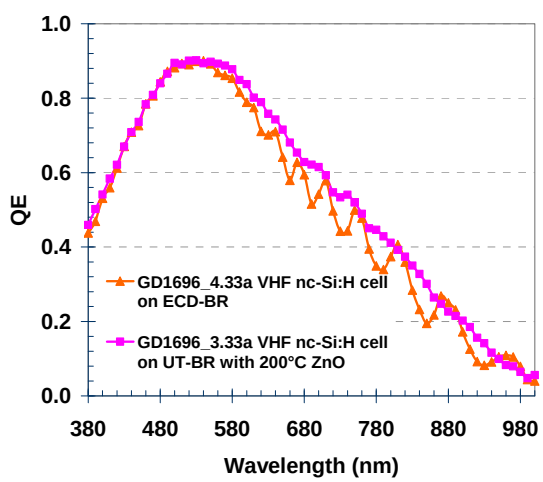

Fig. 6 Quantum efficiency (QE) of nc-Si:H n-i-p solar cells deposited on BR with ZnO films deposited at 280 ºC and on control sample.

Observing the similar performance of nc-Si:H n-i-p single junction cell on BRs with ZnO deposited at 200 ºC and 280 ºC, we decided to fabricate a triple junction a-Si:H/a-SiGe:H/nc-Si:H n-i-p solar cell on a BR with ZnO deposited at 280 ºC. Fig.7 shows the J-V curve of this triple junction cell. High power conversion efficiency of 12.5% is achieved for this case.

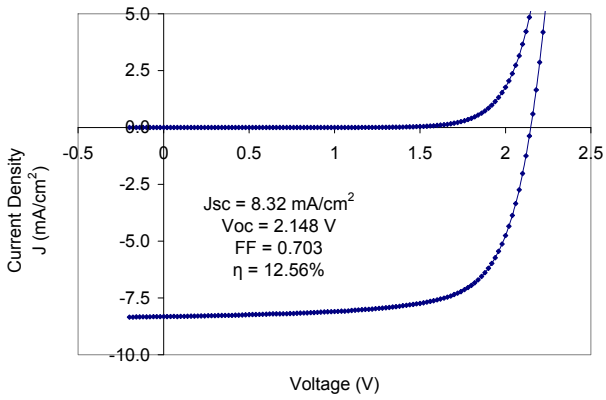

Figure 7. AM1.5 and dark J-V curves of triple junction n-i-p solar cell deposited on BR with ZnO film deposited at 280 ºC.

Figure 8 shows the quantum efficiency data for this triple cell. The QE curve shows that this cell has a good spectral response at the overall wavelength range.

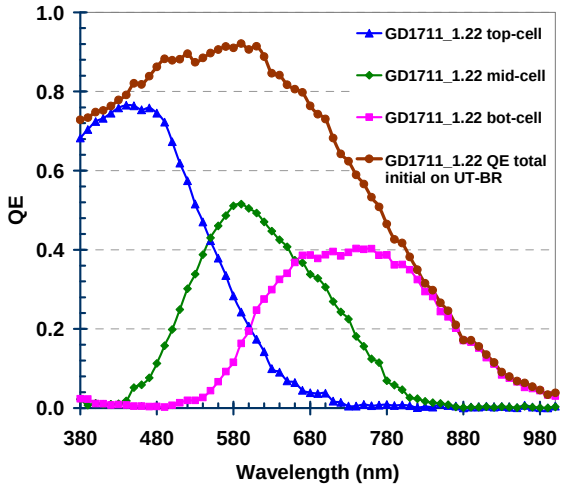

Fig.8 Quantum efficiency (QE) of triple junction n-i-p solar cell fabricated on BR with ZnO film deposited at 280 ºC.

CONCLUSIONS

Nano-crystalline silicon solar cells on BRs with ZnO films deposited at 120 ºC have low FF and low Jsc but high Voc. The reason of this phenomenon may be that the low temperature deposited ZnO films have less crystallinity, which causes the nano-crystalline silicon film to

have more amorphous phase. But when the ZnO is deposited at high temperature (350 ºC), lots of ZnO crystallite rods show up, this can cause yield problem to the solar cells. Based on the BR with ZnO deposited at 280 ºC, we have fabricated a-Si:H/a-SiGe:H/nc-Si:H n-i-p triple junction solar cells with initial efficiency of 12.5%.

ACKNOWLEDGEMENTS

This research was supported by the National Renewable Energy Laboratory "Thin Film Photovoltaics Partnership Program" under subcontract No. ZXL-5-44205-06.

REFERENCES

[1] H. W. Deckman, C.R. Wronski, H. Witzke and E. Yablonovitch, Appl. Phys. Lett. 42, 968 (1983).
[2] X. Deng, K. L. Narasimhan, First WCPEC; Dec. 5-9, 1994; Hawaii.
[3] Kluth, O. Vetterl, R. Carius, F. Finger, S. Wieder, B. Rech, H. Wagner, Mat. Res. Soc. Symp. Rroc. 557 (1999) 731.
[4] B. Rech, H. Wagner, Appl. Phys. A 69 (1999) 155.
[5] J. Koh, Y. Lee, H. Fujwara, C.R. Wronski, R.W. Collins, Appl. Phys. Lett. 73, 1526 (1998).
[6] K. H. Kin, K. C. Park, D. Y. M, J. Appl. Phys. 81 (12) (1997) 7764.
[7] Kluth, B. Rech, L. Houben, S. Wieder, G. Schope, C. Beneking, H. Wagner, A. Loffl, H. W. Schock, Thin Solid Films 351 (1999) 247.